Environmental Science Nano

ROYAL SOCIETY OF CHEMISTRY

PAPER

View Article Online
View Journal

Cite this: DOI: 10.1039/d6en00228e

Key component groups of environment nanoparticles and their corresponding contribution to oxidative stress of *Escherichia coli* in water

Chunlei Jiao,[ab] Tong Sun,[ab] Min Chen,[ab] Yiwei Cai,[ab] Guiying Li [ab] and Taicheng An *[ab]

Received 16th March 2026,
Accepted 25th May 2026

DOI: 10.1039/d6en00228e

rsc.li/es-nano

Environmental nanoparticles (NPs) and microbes are integral parts of natural ecosystems, and they interact inevitably in aquatic environments. However, most previous studies mainly focused on engineered NPs, and the effects and key components of environmental NPs on microorganisms have not been fully clarified. Herein, we collected the environmental NPs from an estuary to study their corresponding effects on growth, cell activity, intracellular reactive oxygen species (ROS), and oxidative stress responses in *E. coli*. Then, the contribution of metal species in the key component of environmental NPs to bacterial oxidative stress was also investigated. Results showed that the environmental NPs could significantly inhibit bacterial growth (25.74–40.35%) and increase intracellular adenosine-triphosphate (ATP) (27.69–62.83%), ROS (2.57–20.72%), and activities of superoxide dismutase (SOD) (65.93–106.33%) and catalase (CAT) (795.47–1600.95%) within 24 h of exposure. Further, the intact morphology of bacterial cells was destroyed, and mRNA levels of oxidative stress, membrane protein, and cell repair genes were upregulated. Asymmetrical flow field-flow fraction (AF4) combined with multiple linear regression analysis showed that the largest size component (843.83 nm) and Al species (followed by Fe, Si, and Zn) in environmental NPs contributed the most to bacterial oxidative stress. Further speciation analysis indicates that the Al species was dominated mainly γ-Al_2O_3. This study provides new insight into the underlying mechanisms and links between environmental NP structure and bacterial oxidative stress in real environmental systems.

Environmental significance

The impact of NPs in the natural environment on microorganisms has long remained an enigma. The main challenge lies in the fact that, unlike the pure engineered NPs commonly used in laboratories, environmental NPs are multi-component, and their impact on microorganisms is also extremely complex. Moreover, exposure concentrations are relatively high in most studies. Therefore, we collected environmental NPs from natural estuaries and studied how they induce oxidative stress in *E. coli* at relatively low concentrations (0.1–10 mg L^{-1}) in water. Additionally, we analyzed the contribution of multiple metal components in environmental NPs to bacterial oxidative stress. This research provides important information for revealing the environmental risks of NPs in real aquatic environments.

1. Introduction

Engineered nanomaterials and their by-products inevitably enter rivers, lakes, estuaries or coastal waters during production, use and waste disposal, which may affect existing habitats and even disturb aquatic biota.[1] There are inevitable biochemical interactions between these metal nanoparticles (NPs) released into the environment or natural mineral NPs and the microorganisms present in the original habitat.[2,3] Generally, microbes are affected by NPs mainly through the following mechanisms: i) reactive oxygen species (ROS) generated at the nano–biological interface could cause oxidative damage to the microbial cells;[4] ii) NPs dissolve and release toxic ions.[5,6] For instance, some NPs with photocatalytic properties could generate holes on their surfaces by photoexcitation, and then react with H_2O or OH–

[a] *Guangdong-Hong Kong-Macao Joint Laboratory for Contaminants Exposure and Health, Guangdong Key Laboratory of Environmental Catalysis and Health Risk Control, Institute of Environmental Health and Pollution Control, Guangdong University of Technology, Guangzhou 510006, China. E-mail: antc99@gdut.edu.cn*
[b] *Guangzhou Key Laboratory of Environmental Catalysis and Pollution Control, Guangdong Basic Research Center of Excellence for Ecological Security and Green Development, School of Environmental Science and Engineering, Guangdong University of Technology, Guangzhou 510006, China*

adsorbed onto the interface to generate ·OH with high oxidative activity. This results in cell membrane rupture and cell death, and even complete decomposition of microorganisms.[4] Ag NPs or Ag_2O NPs have also been shown to release Ag^+ ions that can interact with disulfide or sulfhydryl groups of some biological enzymes in microorganisms, disrupting metabolic processes and ultimately leading to cell death.[6] However, these studies have mostly been conducted with laboratory simulations. NPs undergo complex transformation in the real environmental system (*e.g.*, dissolution/recrystallization, adhesion of organic matter on the surface, *etc.*)[7,8] and thus the interaction mechanism with microorganisms also remains unclear.

The complex speciation of environmental NPs is the main bottleneck in the study of the above problems. Generally, multi-element crystalline cores and organic corona are two of the most typical characteristics of environmental NPs that differ from pure engineered NPs.[9,10] Thanks to advances in analytical techniques and participation of machine learning, research into the association between NP–organic (protein) corona and cell recognition is now extensive.[11] Unfortunately, the biological effects of environmental NP-multi-crystalline cores have not been studied extensively. In the investigation of nanomaterials with high antibacterial and catalytic activities, element doping is a common method. For instance, Ikram *et al.* reported that Ce doping promotes the redshift of bandgap transition in TiO_2 NPs by inhibiting the photogenerated electron–hole pair recombination, and thus improves the antibacterial activity.[12] N/Ag co-doped metal oxide NPs prepared by Wu *et al.* have strong bactericidal activity against *E. coli*, and the mechanism involves oxidative damage in the form of cell wall thinning and cell distortion.[13] Therefore, we hypothesize that environmental NPs could have a non-negligible toxicity on microorganisms, including intracellular ROS generation, inducing oxidative stress and SOS response, where the element composition and abundance in NP-cores are the key factors contributing to the biological effect.

To test this hypothesis, this work mainly investigated the influence of environmental NPs from urban estuarine areas on the physiological and biochemical status of *E. coli*, and analysed the key components and dominant metal species. Then, NP-components and their elemental abundances in the environmental NPs in estuary were investigated by asymmetrical flow field-flow fractionation combined with multi-angle light scattering and inductively coupled plasma mass spectrometry (AF4-MALS-ICP-MS). In addition, the correlation and contribution of the above environmental NP structural features to the oxidative stress of *E. coli* were analysed integrating multiple linear regression with *in situ* crystal analysis. The information obtained offers new insights into key structural and component features of NPs regarding exposure risk involved in real environmental systems.

2. Materials and methods

2.1 Extraction and separation of environmental NPs

Yingzai Bay, an important bay and the estuary of many rivers in the Beibu Gulf of the South China Sea, with great potential to enrich environmental NPs, was selected as a sampling area. Water samples (50 L in total) were collected in June 2023 at 109.85°E, 21.45°N. To ensure representation, water was collected at 0.5 m below the surface water from three random places and thoroughly mixed evenly. The samples were filtered through a filter membrane (1 μm), then NPs in water were concentrated, demineralized and separated multiple times in an intelligent tangential flow filtration (TFF) system (Challenge IM, China). The detailed operation process is provided in Text S1. Finally, suspensions of environmental NPs ranging from 10–100 kDa, 100–1000 kDa, and 1000 kDa–1 μm were obtained and named as Sample A, Sample B, and Sample C, respectively, which were used in subsequent bacterial exposure experiments.

2.2 Characterization of environmental NPs

The total element concentrations of all the environmental NP suspensions were determined using ICP-MS (NexION 300X, PerkinElmer, USA) after digestion with *aqua regia*. Detailed digestion procedures are provided in Text S2. The environmental NP suspension was dropped onto a clean silicon wafer. After drying and gold spraying, the surface morphology and element distribution mapping of resultant environmental NPs were measured using scanning electron microscopy (SEM, SU8010, Hitachi, Japan) and its associated energy dispersive spectroscopy (EDS) at an accelerating voltage of 10 kV. The morphology, semi-quantitative elemental analysis and crystallinity of environmental NPs were investigated with a JEM-F200 high resolution transmission electron microscope (TEM, JEOL, Japan) at an accelerating voltage of 200 kV combined with EDS. The pH values of environmental NP suspensions were adjusted to 2.0–12.0, and samples were oscillated at 200 rpm for 6 h at 25 °C in an orbital shaker. The zeta potential and hydrodynamic size of resultant environmental NPs were analysed using dynamic light scattering (DLS, Zetasizer NANO ZS, Malvern, UK).

AF4 uses a hollow, flat separation channel that applies a separation force in a direction perpendicular to the sample stream. Here, the hydrodynamically active (generally small size) components are first detected by the back-end detector, while the hydrodynamically lazy (generally large size) components are then detected to achieve the purpose of separation. AF4 technology was used in combination with MALS (Postnova, Germany) and ICP-MS (7900, Agilent, USA) to characterize the colloidal properties of NPs in electrolyte solutions to evaluate NP compositions and key element abundances of the environmental NPs. A polyethersulfone membrane (1 kDa) and carrier solution (10 μM NaCl) were used during AF4 measurement. For fractionation of the above-mentioned Sample A, B, and C, 1 mL sample was injected at a cross-flow of 3 mL min^{-1} with a focus time of 20 min. Then

the particles were separated by a linear cross-flow decrease for 40 min. The largest particles were flushed last at a constant cross-flow of 10 mL min^{-1} for 20 min. The fitting curve of NP-hydrodynamic size and residence time for AF4 separation was obtained using latex standards with sizes of 20, 200, 596, and 900 nm (from Postnova Analytics). Data from ICP-MS were analysed in Origin 2018 (OriginLab, USA). The residence time of all the NP compositions in a sample was located according to the peak position of the MALS spectrum. Base correction and peak area calculation were performed for all ICP-MS spectra with the above residence time. The elemental abundance of all compositions on every environmental NP sample was obtained.

2.3 Bacterial culture and batch exposure

E. coli, a classic model microbe, was selected to test the microbial effects of environmental NPs. *E. coli* K-12 were cultured overnight in Luria-Bertani medium at 37 °C and 180 rpm then washed and suspended three times with normal saline. Stable growth curves were tested for *E. coli* in normal saline to assess the viability and growth.[14] Then, the bacteria were used for batch exposure experiments and mechanism studies.

The effects of three groups of environmental NPs (Sample A, B and C) on microbial physiology and biochemistry were investigated under different concentrations (measured as total element concentration: 0, 0.1, 0.5, 1, 5, and 10 mg L^{-1}) and exposure times (0, 1, 6, 12, and 24 h). In addition, bacteria not exposed to any environmental NPs were set as the control group. All experiments were performed in a saline system with a microbial concentration of 1×10^9 CFU mL^{-1}.

2.4 Detection of bacterial physiological and biochemical properties

2.4.1 Growth and cell activity. The Luria-Bertani agar plate counting method was used to measure bacterial concentrations after exposure and in controls.[3] The intracellular adenosine-triphosphate (ATP) level was detected using an ATP Assay kit (S0026, Beyotime Biotechnology, China).[15] The detailed procedures are shown in Text S3. All the samples were analysed in triplicate.

2.4.2 Intracellular ROS levels. The DCFH-DA dye (S0033S, Beyotime, China) was used to stain bacterial cells and detect the intracellular ROS level after exposure to environmental NPs as provided in Text S3. All the samples were analysed in triplicate.

2.4.3 Enzymatic activity. *E. coli* cells were harvested from 2.0 mL of bacterial cell suspension. The bacterial suspension was lysed with a bacterial protein extraction kit (C600596, Sangon Biotech, China), and then the supernatant was collected for testing of protein concentration and subsequent enzymatic activity. The activities of superoxide dismutase (SOD), catalase (CAT), and glutathione peroxidase (GSH-Px) were measured with a total superoxide dismutase assay kit with WST-8 (S0101S, Beyotime, China), catalase assay kit (S0051, Beyotime, China), and total glutathione peroxidase assay kit with NADPH (S0058, Beyotime, China), respectively. All enzymatic activities were normalized by protein concentration, which was detected by the BCA protein assay kit (P0012S, Beyotime, China). All the samples were analysed in triplicate. The detailed procedures are shown in Text S3.

2.5 Assessment of bacterial morphology under environmental NP stress

The bacterial cell structure was observed by SEM (Sigma300, Zeiss, Germany) under different treatments. The adsorption of NPs on the bacterial cell surface and cellular damage were characterized by TEM (HT7700, Hitachi, Japan).[16] The detailed procedures are shown in Text S4.

2.6 Measurement of mRNA expression of stress response-coding genes

To clear the mechanism of environmental NPs induce microbial oxidative stress and SOS response, the expression of genes related to oxidative stress regulatory, cell repair, DNA repair, outer membrane functional protein, protein/folate/DNA/RNA synthesis, flagellar and chemotaxis was evaluated by qPCR analysis. The 16S rRNA gene was used as an internal control.[17] The gene information and primer sequences are provided in Table S1 and the detailed procedures are shown in Text S5.

2.7 Statistical analysis

All statistical analyses were carried out using the Statistical Package for the Social Sciences 19.0 (SPSS, Chicago, USA). After exposure to different concentrations and times of environmental NPs, significant differences in bacterial growth number, intracellular ATP, ROS, and antioxidant enzyme activity were assessed using the one-way analysis of variance (ANOVA) and LSD test at a significance level of $p = 0.05$. $p < 0.05$ means statistically significant. To assess the correlation between structural features of environmental NPs (*i.e.*, NP-component and its key element abundance) and the above indicators of bacteria, we employed Pearson's correlation analysis using Python's Pandas library. Additionally, to analyse the contribution of multiple features of environmental NPs to cytotoxicity, we employed the multiple linear regression method to perform regression analysis on the two datasets and obtained the contribution values of different features.

3. Results and discussion

3.1 Characteristics of environmental NPs from estuarine waters

The environmental NPs in estuarine waters showed irregular microstructure (Fig. S1A), almost consistent with previous studies.[3] Both natural mineral NPs and engineered NPs released into the environment usually form various

unpredictable structures under the influence of complex environmental conditions and media. Simultaneously, the surface of environmental NPs adheres to uncertain-shape substances, which may be the environmental corona formed by natural organic matter.[18] According to the EDS analysis and element mapping (Fig. S1B and C), C, P and S were rich on the surface of environmental NPs. This is mainly attributed to the fact that environmental crowns are generally composed of organic matter formed after biomass degradation.[9] After *aqua regia* digestion and ICP-MS detection, the core elements of environmental NPs were concentrated in Sn, Si, Sb, Fe, Zn, Bi, Al, Mo, *etc.* with low environmental concentrations (0.031–0.259 mg L^{-1}) (Table S2). Additionally, considering that metal sulfides are important sinks for multiple metal elements in real environmental systems, the high abundance of S element may also originate from the sulfides of the aforementioned metals (*e.g.*, FeS_2, FeS, and ZnS).[19] In addition, although environmental NPs have complex composition and surface structure, they still maintain basic colloidal properties and stability. After long-term incubation and surface modification of natural organic matter, the surface of mineral NPs is usually negatively charged (Fig. S1D), which could promote their electrostatic stability and lead to the weakening of their agglomeration trend.[20] Particularly, the attractive force is more dominant around the point of zero charge, resulting in environmental NPs' instability and high agglomeration rate.[21] An increasing trend of aggregation and sedimentation (hydrodynamic size) of environmental NPs in solution was found as the repulsive barrier was close to zero. Overall, the environmental NPs were regarded as a typical colloidal structure with a multi-element crystalline core and P/S organic matter corona.

Important parameters, such as hydrodynamic size, NP-component, and its key element abundance, affecting the biological effects of samples A, B, and C separated from environmental NPs by TFF were compared. Generally, the environmental behaviors of NPs depend on their hydrodynamic properties in electrolyte solutions.[22] In this study, environmental NPs were separated into samples A, B, and C according to their molecular weight based on the TFF operating index, but the hydrodynamic sizes of the three samples were slightly different and not significant (Table S3). The MALS and ICP-MS spectra with AF4 showed these three groups of samples with different residence times (Fig. 1). Here, each peak represents a class of environmental NP-components with similar hydrodynamic migration properties. As shown in MALS spectra, each sample presents 6 characteristic peaks corresponding to 6 key NP-components. Meanwhile, each NP-component contains 4 key elements (Al/Si/Fe/Zn) from ICP-MS spectra after excluding the spectrum of elements with excessive noise or weak NP signals (Fig. S2). The integral concentrations of key elements in each NP-component are presented in Table S2. The Al-, Si-, Fe-, and Zn-containing NPs might be derived from natural mineral NPs, such as bauxite, silicate mineral, goethite/hematite, and sphalerite, or corresponding

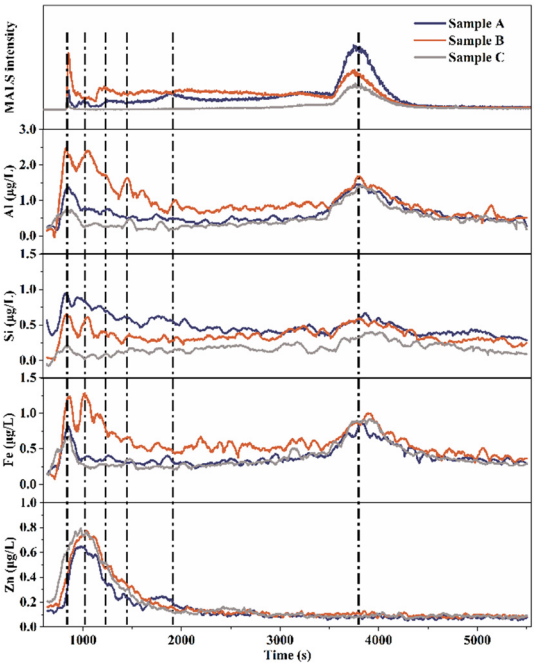

Fig. 1 AF4 fractograms involving MALS intensity and key element (Al/Si/Fe/Zn) concentration. The dotted line indicates the residence time (peak location) of the AF4 system corresponding to the key NP group. The integral concentrations of key element (Al/Si/Fe/Zn) peaks of each NP group are presented in Table S3.

engineered NPs, such as Al_2O_3, SiO_2, Fe_2O_3, and ZnO NPs. These metal-based engineered NPs are the most commonly reported species with potential health risks and hazardous effects.[23] Therefore, the above metal-containing NP-components from estuarine waters may be the key components to inducing microbial oxidative stress.

3.2 Effects of environmental NPs on the physiology and biochemistry of bacteria

To assess whether the above environmental NPs induce oxidative stress in bacteria, bacterial growth, cellular ATP, intracellular ROS production, and antioxidant enzyme activity were systematically evaluated during continuous exposure to different environmental NP samples. As Fig. 2A shows, 10 mg L^{-1} environmental NPs had significant growth inhibition compared with the control only at the initial (1 h) and late (24 h) stages of exposure ($p \leq 0.05$). Noteworthily, the initial growth inhibition was mainly caused by low molecular weight samples A and B (40.35%, 25.74%), in contrast to the late inhibition caused by the large molecular weight Sample C (34.78%). The changes of intracellular ROS could indicate oxidative stress occurrence in bacteria. During exposure to each environmental NP sample, the intracellular ROS of *E. coli* increased slightly (2.57–20.72%), among which only Sample B exposure could induce significantly oxidative stress compared to the control (Fig. 2B). Among some proposed mechanisms of action of metal NPs on bacterial cells, one is the induction of oxidative stress by the generated ROS.[24]

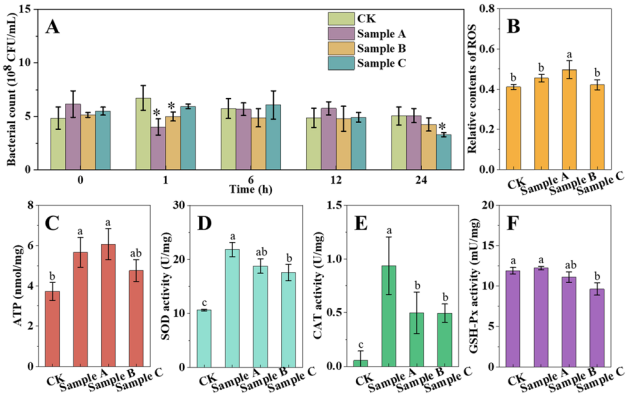

Fig. 2 (A) Time–growth curves of *E. coli* treated with 10 mg L^{-1} environmental NP samples. (B) Intracellular ROS, (C) cellular ATP, and (D–F) antioxidant enzymatic activities of *E. coli* cells treated with 10 mg L^{-1} environmental NP samples for 24 h. Data are average of three replicates ± standard deviations. * indicates a significant difference between the exposure and control groups (CK) under the same exposure conditions ($p \leq 0.05$). Different letters stand for statistical differences between treatments at $p \leq 0.05$.

Overall, the bacterial toxicity of environmental NPs was not heavy in terms of bacterial growth and ROS production, which might be attributed to the low-dose NP-exposure in this study. Furthermore, NPs have undergone sufficient aging processes in natural environmental systems, especially elemental doping in the core and environmental corona formation on the surface, which may further reduce the toxicity of NPs.[25] Additionally, intracellular ROS induced by metal NPs include $O_2^{\bullet-}$, $^{\bullet}OH$, H_2O_2, and $^1O_2$.[26] Different NPs or combinations of NPs could induce various types of intracellular ROS, and therefore the resulting toxic manifestations of bacteria are also different.

Generally, intracellular ROS production induced by metal NPs is accompanied by the oxidative stress process of bacteria.[27] The interaction of NPs with bacterial outer layers, or ROS can disturb electron transport, cellular respiration, and the ATP level.[28,29] Most metal NPs can cause a decrease in cellular ATP, which is attributed to the disturbances of the cell membrane, and the stimulated cascade mechanism of ROS-induced oxidation–reduction reactions could result in ATPase inactivation.[30,31] However, this study found that exposure to environmental NPs increased ATP concentration in *E. coli* cells (27.69–62.83%). Particularly, ATP significantly increased in the groups exposed to samples A and B ($p \leq 0.05$) (Fig. 2C). The change in antioxidant enzyme activity is another important indicator of bacterial oxidative stress. The microbial defense system against the harmful effect of NPs and ROS consists of CAT and SOD together with a non-catalytic antioxidant (GSH-Px).[26] As Fig. 2D and E show, the SOD and CAT activities of *E. coli* significantly increased in the three exposure groups (65.93–106.33%, 795.47–1600.95%), especially in Sample A (the smallest molecular weight). In contrast, the GSH-Px activity of *E. coli* decreased under exposure to Sample C (Fig. 2F). SOD, CAT, and GSH-Px have the function of scavenging different free radicals in bacteria, corresponding to $O_2^{\bullet-}$, H_2O_2 and glutathione (GSH)/H_2O_2, respectively.[3,32] These may imply that ROS produced by *E. coli* induced by environmental NPs are mainly derived from $O_2^{\bullet-}$ and H_2O_2. Meanwhile, SOD could catalyse the disproportionation reaction of $O_2^{\bullet-}$ to produce H_2O_2 and O_2, which further increases the level of intracellular H_2O_2, thus inducing bacteria to produce more CAT.

In addition to the biochemical damage pathway mediated by ROS, the mechanical mechanism by which environmental NPs impede the transmembrane material transport by attaching to the bacterial surface may be another pathway causing bacterial growth inhibition.[3] This process was particularly evident in the interaction between Sample C and bacteria. Compared with other samples, Sample C exhibited slower antibacterial effects, accompanied by reduced levels of ROS, ATP, and antioxidant enzyme activities (Fig. 2). Compared with samples A and B, it might be more difficult for Sample C with a higher molecular weight to enter the cells rapidly. The environmental NPs in Sample C might mainly exert antibacterial effects by continuously attaching to the bacterial surface, which gradually impedes the transmembrane material transport. Eventually, the bacterial division and growth were mechanically inhibited, manifested as significant growth inhibition (34.78%).

3.3 Oxidative stress in bacteria under the influence of environmental NPs

Sample A with the most significant microbial effect was taken as an environmental NP example to further explore the mechanism of oxidative stress and SOS response induced by environmental NPs. The intracellular ROS generation was in a dose-dependent trend, with the low (0.1 mg L^{-1}) and high doses (5 or 10 mg L^{-1}) environmental NPs promoting intracellular ROS production while medium doses (0.5 or 1

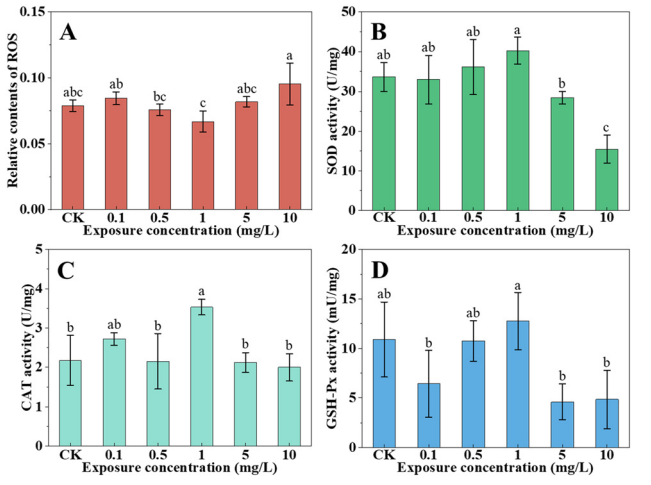

Fig. 3 (A) Intracellular ROS, (B) SOD, (C) CAT, and (D) GSH-Px activities of *E. coli* treated with 0–10 mg L^{-1} Sample A for 24 h. Data are average of three replicates ± standard deviations. Different letters stand for statistical differences between treatments at $p \leq 0.05$.

mg L^{-1}) showed the opposite effect, but neither was significant compared to the control (Fig. 3A). Several works have proven that metal compositions in NPs could induce ROS generation, which is tightly integrated with lipid peroxidation, oxidative stress, and bacterial cell structure changes.[33,34] We did find membrane damage and changes in cell structure of bacteria under environmental NPs stress (Fig. S3). Compared with the control, *E. coli* cell bodies after exposure to 10 mg L^{-1} environmental NPs for 24 h had obvious morphological deformation, collapse, or surface damage. Meanwhile, adsorption of a large number of NPs onto the bacterial surface and the development of biofilms between colonies were clearly observed. Various metal-based engineered NPs can inhibit bacterial growth and bacterial biofilm formation.[35,36] Usually, biofilms exist in various environments, serving as protection from environmental stress.[19]

Oxidative stress refers to a state of imbalance between oxidation and antioxidant action in bacterial cells. To examine the functioning of the antioxidant system in bacterial cells, the activity of the primary antioxidant enzymes, including CAT, SOD, and GSH-Px, was also evaluated at different exposure doses and times of environmental NPs. In Fig. 3B–D, SOD, CAT, and GSH-Px activities of bacteria were also dose-dependent. That is, NPs with low (0.1 or 0.5 mg L^{-1}) and high concentrations (5 or 10 mg L^{-1}) inhibited enzyme activity, while medium concentration (1 mg L^{-1}) promoted enzyme activity. Among them, only 10 mg L^{-1} of environmental NPs showed a significant inhibition on SOD activity, while 1 mg L^{-1} of that significantly promoted the CAT and GSH-Px activities. A low level of intracellular ROS was always accompanied by high levels of antioxidant enzyme activity under the same NP-exposure dose, and *vice versa*. Engineered metal-based NPs including Ag, Cu, ZnO, TiO_2, and Fe_3O_4 NPs have similar effects.[37,38] It might be the relationship between ROS generation and the functioning of the antioxidant defense system. The antioxidative enzymes would clear the rapidly elevated intracellular ROS (*e.g.*, $O_2^{\cdot-}$, H_2O_2) to protect cells against oxidative stress. Notably, low dose NP-exposure might have no significant biological toxicity, while mid-dose NPs were exactly the threshold for inducing oxidative stress in bacteria. The interaction of NPs with bacterial outer layers, or ROS can lead to a disturbance of biochemical processes, including cellular respiration and electron transport.[28,29] When the dose of NPs exceeds the threshold that bacteria can tolerate, lots of antioxidant enzymes will lose their activities, producing protein fragments and protein carbonyl derivatives.[39] In such a state of stress, bacterial activity dropped to the lowest among all exposure groups (Fig. S4A). It may also be that the level of ROS generated overpowered the antioxidative ability of these enzymes.[3]

The above results illustrated the outcome of bacterial oxidative stress, but the process was not well understood. Therefore, the intracellular ROS and antioxidant enzyme activities under environmental high dose NP-exposure on a time gradient were explored. As shown in Fig. S5A, the intracellular ROS of *E. coli* first increased and then decreased slowly with the continuation of exposure, and only the ROS level at 1 h NP-exposure was significantly higher than those at 12 h in all exposure groups. Comparatively, SOD and CAT activity levels showed trends similar to that of intracellular ROS, while the GSH-Px activity first rose and then fluctuated with exposure time prolonging (Fig. S5B–D). Based on previous inferences, *E. coli* had exceeded the threshold at which its antioxidant system could cope with the stress with 24 h exposure to the high dose of environmental NPs. Thus, it was reasonable that *E. coli* underwent initial oxidative stress and eventual oxidative damage as exposure continued. This conclusion was also supported by the decrease of cellular ATP at the later stage (6–12 h) of the exposure time gradient (Fig. S4B).

Generally, the intracellular ROS production induced by metal NPs is accompanied by oxidative stress and SOS response of bacteria.[27] Oxidative stress regulatory, DNA repair, outer membrane functional protein, folate/DNA/RNA synthesis, and quorum sensing genes have been proven to play key roles in bacterial oxidative stress, SOS response, and membrane function.[40] As shown in Fig. 4, at the initial stage (1 h) of NP-exposure, the expressions of all target genes were upregulated. Notably, expressions of oxidative stress regulatory (*osmY*, *soxR*), DNA repair (*ruvB*, *rpoD*), outer membrane functional protein (*ompA*), folate synthesis (*folA*), and quorum sensing (*lsrk*) genes all increased by 2–27-fold, 3–16-fold, 3-fold, 4-fold and 5-fold, respectively. Stress-response genes coordinate antioxidant defense and cellular signaling in *E. coli*.[41] The elevated expression levels were consistent with increased intracellular ROS production (Fig. S5A), indicating activation of oxidative stress responses. Upregulation of folate synthesis genes further suggests

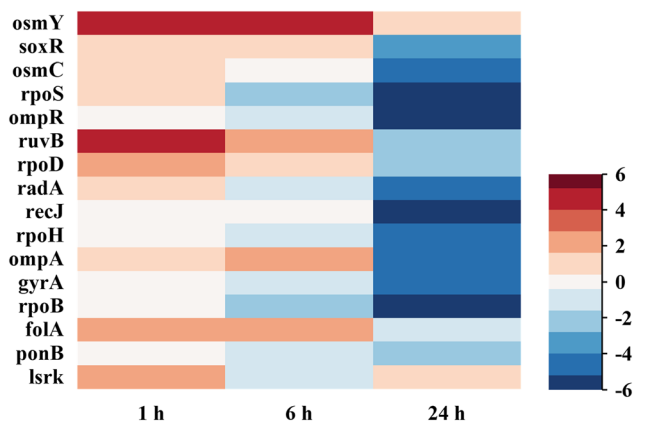

Fig. 4 Gene expression profiles of target genes involved in oxidative stress regulatory, cell repair, DNA repair, outer membrane protein-encoding genes, protein/folate/DNA/RNA synthesis, flagellar and chemotaxis upon exposure to environmental NPs in *E. coli* under 1, 6, and 24 h. *X*-Axis: the monitoring time in hours; *Y*-axis left: clusters of target genes and list of genes tested, *Y*-axis right: the figure legend bar depicted as a green-red color scale. The red spectrum indicates upregulated expression; the blue spectrum indicates downregulated expression.

enhanced metabolic activity to support biomolecule synthesis under stress conditions.[42]

At the middle stage (6 h), oxidative stress-related and folate-related genes remained elevated (3–25-fold), indicating sustained stress. DNA damage caused by ROS likely triggered the bacterial SOS response, as reflected by continued upregulation of DNA repair genes.[43] The accumulation of single-stranded DNA acts as a genotoxic signal that activates SOS pathways to facilitate DNA repair.[44] In addition, the above observed membrane damage and biofilm formation (Fig. S3B) under NP stress might be associated with increased expression of outer membrane protein (*ompA*)[45] and quorum sensing (*lsrk*) genes.[46] Previous studies have demonstrated a close relationship between oxidative stress and biofilm formation on metal interfaces.[17,47] Furthermore, increased gene expression also reflects active bacterial responses to external stimuli.[3] Consistently, a significant increase in intracellular ATP levels was found at 6 h, indicating elevated metabolic activity during NP exposure (Fig. S4B).

At the late stage of exposure (24 h), the expressions of all target genes were downregulated, indicating that the bacteria might be damaged and the bacterial defense system was destroyed by ROS. Based on previous inferences, *E. coli* had exceeded the threshold at which its antioxidant system could cope with stress after 24 h exposure to a high dose of environmental NPs. Meanwhile, antioxidant enzyme activities and bacterial activity were significantly reduced (Fig. S4, S5B, and C), and bacterial cell membranes were damaged (Fig. S3B and D). Overall, similar to the mechanism by which engineered metal-based NPs induce bacterial oxidative stress, environmental NPs directly produce high concentrations of ROS in cells through adsorption to the surface of cell membranes or ingestion by bacteria, thereby causing bacterial oxidative stress and damaging various bacterial biomolecules (*e.g.*, cell membrane, DNA). The antioxidative enzymes would clear the rapidly elevated intracellular ROS to protect the cells against oxidative stress. Meanwhile, bacteria upregulated the gene expression of oxidative stress, DNA repair, membrane functional protein, and quorum sensing through SOS response, began to cope with the damage of ROS to the cell membrane and DNA, and produced biofilms. However, after sustained exposure to high doses of environmental NPs, bacteria reached the limit of their ability to resist external stress, the antioxidant system completely collapsed, and the expression of the above genes was downregulated across the board.

3.4 Identification of key NP-components to bacterial oxidative stress

The metal components in the environmental NP core may be the key to inducing oxidative stress in bacteria. The Pearson's correlations between 6 key NP-components and their 4 key elements in environmental NPs and physiological and biochemical indicators in bacteria demonstrate the close relationship between environmental NPs and bacterial oxidative stress (Fig. S6). Among them, the growth of bacteria at 0/12 h, cellular ATP, intracellular ROS and SOD/CAT antioxidant enzymatic activities were identified as sensitive indicators in response to environmental NP-components ($r \geq 0.8$, $p < 0.05$). Based on the above sensitive indicators, the contributions of 6 key NP-components and their 4 key elements in environmental NPs to bacterial oxidative stress were further calculated. As shown in Fig. 5, the contribution of different components in environmental NPs to bacterial oxidative stress varied, among which Comp. 6 had the largest total contribution. The environmental NPs with small size were more concentrated on low residence time than those with large particle size in AF4, meaning that Comp. 6 had the largest particle size (843.83 nm, Table S3 and Fig. S7) of all the NP-components. It is noteworthy that although the pretreatment protocol preserved native NP structures by minimizing physicochemical alterations, environmental NPs were inherently meta-stable assemblages. Changes in the environmental medium (*e.g.*, ionic strength) during the pretreatment and fractionation processes might induce colloidal dispersion or aggregation. Generally, the biological toxicity of engineered NPs increases with the decrease of their particle size.[48] It might be that smaller particle size NPs generally have a higher specific surface area, surface activity, and specific charge, which are easier to be adsorbed by the bacterial membrane surface or ingested by bacteria and produce high levels of intracellular ROS. However, the environmental NPs with multi-components used in this study did not fit into the conclusions obtained in previous studies using pure engineered NPs. This contradiction also supported the original hypothesis that it might be difficult for laboratory simulation studies to accurately describe the interaction between NPs and microorganisms in real environmental systems.

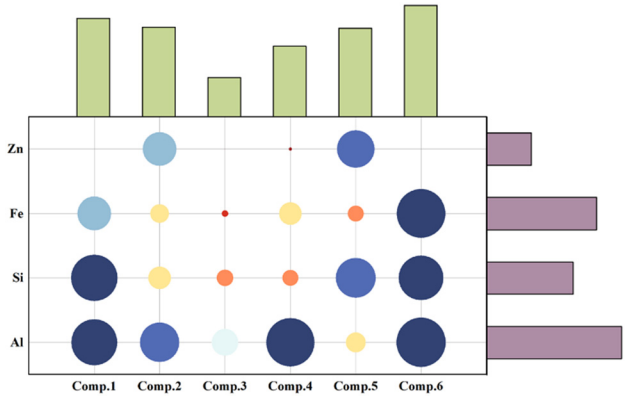

Fig. 5 Contribution of key NP-components and their elements in environmental NPs to bacterial oxidative stress. The contribution values of multiple features of environmental NPs were obtained by multiple linear regression. The size of the bubble corresponds to the level of contribution; the top and right columns correspond to the total contribution of key components or key elements, respectively.

The chemical composition and speciation of NP-components might be the key factor to the biological effect of environmental NPs. As shown in Fig. 5, the Al element contributed the most to bacterial oxidative stress in most components (*i.e.*, Comp. 2, 3, 4, 6), followed by Fe, Si, and Zn. Al_2O_3 NPs belong to the list of 13 representative reference nanomaterials selected by the OECD Working Party on Manufactured Nanomaterials. The bactericidal properties of Al_2O_3 NPs have been widely reported. For instance, Jiang *et al.* found that 20 mg L^{-1} commercial Al_2O_3 NPs (60 nm) have a mortality rate of 36% to *E. coli*.[49] Simon-Deckers *et al.* found that commercial Al_2O_3 NPs (11 nm) at 10, 100, and 500 mg L^{-1} induce a significant loss of viability in *E. coli* MG1655.[50] In this study, we observed some α-Al_2O_3 on the NP-component rich in Al species, due to their characteristic lattice plane (110). In addition, there was boehmite (γ-$Al_2O_3{\cdot}H_2O$, or AlOOH), involving multiple characteristic lattice planes, such as (021), (130), and (002), and bits of bayerite ($Al(OH)_3$) lattice plane (021) (Fig. 6). Crucially, comprehensive compositional analysis of morphologically analogous environmental NPs revealed an average O content of 56.0 ± 1.7% (mean ± SD, n = 3) (Fig. S8A). The elevated O content might indicate that environmental NPs are heterogeneous composites (Al_2O_3 with 47.06% O). These particles likely contain symbiotic minerals—such as silicates (*e.g.*, SiO_2 with 53.3% O) or hydrated phyllosilicates (*e.g.*, halloysite with 59.9% O)—which collectively contribute to their complex O signature. Utilizing TEM to observe the lattice spacings of more NPs, the characteristic lattice planes, such as (021) and (1,−1,0), of halloysite were indeed discovered (Fig. S8B). The α-Al_2O_3 phase is the only thermodynamically stable form of Al_2O_3, and the most commonly occurring modification of Al_2O_3 also known as alumina in nature. Together with silica, α-Al_2O_3 constitutes the fundamental backbone of clay-forming minerals.[51] Serdar *et al.* showed that γ-Al_2O_3 causes oxidative stress of *Gammarus pulex* earlier, and a higher level of unsaturated fatty acid peroxidation than α-Al_2O_3.[52] Pakrashi *et al.* demonstrated a higher antibacterial activity of γ-Al_2O_3 than α-Al_2O_3 against *Bacillus licheniformis* after 2 h exposure, which is manifested in a higher level of ROS after exposure to γ-Al_2O_3 compared to α-Al_2O_3.[53] Differences in atomic arrangement lead to variations in reactivity that may affect toxic properties. The oxygen sublattice in α-Al_2O_3 is a hexagonal-close-packed structure, where two-thirds of the sites are occupied with cations, while γ-Al_2O_3 has a face-centered cubic orientation, with oxygen atoms and cations present in different proportions in octahedral and tetrahedral sites.[54] Therefore, the γ-Al_2O_3 with high abundance might be the key species in the Comp. 6 of environmental NPs.

It is worth noting that the NP exposure threshold identified in this study (≤10 mg L^{-1}) for inhibiting growth and causing oxidative stress of *E. coli* was significantly lower than that found in previous studies (100–100 000 mg L^{-1}).[55,56] Moreover, the exposure concentration was not the concentration of Al_2O_3 NPs, but the total elemental concentration of all environmental NPs. Besides the key species (*e.g.*, γ-Al_2O_3) that could induce bacterial oxidative stress, the potentially synergistic interactions among multiple components in environmental NPs were also likely the key to their significant microbial effects. This mechanism was particularly evident in Comp. 6. As shown in Fig. 5, the contribution value of Fe was close to that of Al, suggesting that Fe species (likely Fe_2O_3 or Fe_3O_4, as evidenced by TEM in Fig. S9) might form a synergistic effect with Al species. Liu *et al.* enhanced the photoelectrocatalytic performance of α-Fe_2O_3 thin films by integrating Au NPs and Al_2O_3 by surface passivation, achieving a 1.78-fold increase in efficiency through localized surface plasmon resonance and effective charge transfer mechanisms,[57] which aligns with the similar Al/Fe contribution patterns observed in our study. The prolonged utilization of a single type of NPs may result in an elevation of bacterial adaptability. Nevertheless, bacteria encounter difficulties in concurrently developing resistance to multiple attack strategies within a mixed system owing to the diverse modes of action. Chen *et al.* constructed a ZnO@Ag-functionalized paper-based microarray chip, confirming that the photocatalytic ROS production ability of ZnO and the membrane-damaging effect of Ag^+ formed a synergistic amplification effect.[58] Baláž *et al.* synthesized some ternary/quaternary copper-based sulfide nanocrystals (*e.g.*, Cu_2FeSnS_4, Cu_2ZnSnS_4) through a mechanochemical method. Their antibacterial mechanism lies in the interference of metal ions ($Cu^+/Fe^{2+}/Zn^{2+}/Sn^{4+}$) with the respiratory chain and the oxidation of protein sulfhydryl groups by sulfhydryl radicals (·SH), forming a non-antibiotic-dependent killing pathway.[59] The inherent multicomponent nature of environmental NPs implies that

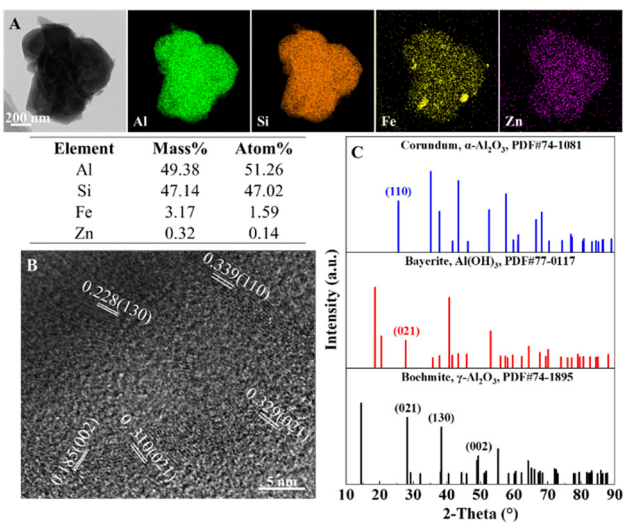

Fig. 6 (A) Micromorphology, key elemental mapping and percentage content of Al-containing components in environmental NPs; (B) the lattice spacing and crystal plane parameters of Al species crystals in Al-containing components; (C) XRD patterns of the standard samples of Al-containing crystals (*i.e.*, corundum, bayerite, and boehmite) which were exported from the standard powder card in Jade 5.0 (MDI, California, USA).

inter-component synergy likely serves as a primordial regulatory mechanism in NP–microbiota interfacial dynamics. Nevertheless, direct validation of synergy (*e.g.*, *via* binary mixture assays) remains a future research direction.

Conclusions

This study mainly investigated contributions and mechanisms of various components of environmental NPs extracted from urban estuaries to the oxidative stress of *E. coli*. The surface adsorption and intracellular uptake of NPs by bacteria could significantly induce oxidative stress processes, such as ROS production and enhancement of antioxidant enzyme activity, as well as the upregulation of the expression of genes related to oxidative stress, membrane protein, and cell repair. Interestingly, in contrast to the conventional wisdom that NPs with smaller particle sizes are more toxic, the largest components in environmental NPs contributed the most to the above process. The high abundance of γ-Al_2O_3 in the NP-component and the synergistic effect among multiple components may be the key factors explaining this unique phenomenon. We speculated that species composition, rather than size for multi-component environmental NPs, determines the biological effects. These findings reveal that the key components of environmental NPs induced microbial effects in natural water, filling the gaps in the general interaction between environmental NPs and microorganisms in geochemical processes.

Author contributions

C. Jiao: investigation, formal analysis, writing – original draft, funding acquisition. T. Sun: investigation, formal analysis. M. Chen: investigation. Y. Cai: investigation and methodology. G. Li: writing review & editing, resources, funding acquisition. T. An: conceptualization, writing review & editing, resources, funding acquisition.

Conflicts of interest

There are no conflicts to declare.

Data availability

The data supporting this article have been included as part of the supplementary information (SI).

Supplementary information is available. See DOI: https://doi.org/10.1039/d6en00228e.

Acknowledgements

The author would like to acknowledge the financial support from the National Natural Science Foundation of China (42330702 and 42407300), Introduction Innovative and Research Teams Project of Guangdong Pearl River Talents Program (2023ZT10L102), and Guangdong Basic and Applied Basic Research Foundation (2023A1515111134). Special thanks are extended to Dr. Miaoyue Zhang and Dr. Quan Wan from Sun Yat-sen University for their expert technical assistance with AF4 and its coupling techniques.

Notes and references

1 M. Arienzo and L. Ferrara, Environmental Fate of Metal Nanoparticles in Estuarine Environments, *Water*, 2022, **14**, 1297.
2 A. Lu, Y. Li, S. Jin, X. Wang, X.-L. Wu, C. Zeng, Y. Li, H. Ding, R. Hao and M. Lv, Growth of non-phototrophic microorganisms using solar energy through mineral photocatalysis, *Nat. Commun.*, 2012, **3**, 768.
3 G. Li, X. Chen, H. Yin, W. Wang, P. K. Wong and T. An, Natural sphalerite nanoparticles can accelerate horizontal transfer of plasmid-mediated antibiotic-resistance genes, *Environ. Int.*, 2020, **136**, 105497.
4 A. Khezerlou, M. Alizadeh-Sani, M. Azizi-Lalabadi and A. Ehsani, Nanoparticles and their antimicrobial properties against pathogens including bacteria, fungi, parasites and viruses, *Microb. Pathog.*, 2018, **123**, 505–526.
5 X. Wang, H. Dong, Q. Zeng, Q. Xia, L. Zhang and Z. Zhou, Reduced iron-containing clay minerals as antibacterial agents, *Environ. Sci. Technol.*, 2017, **51**, 7639–7647.
6 O. V. Morozova and D. V. Klinov, Nanosilver in Biomedicine: Advantages and Restrictions, in *Silver Micro-Nanoparticles-Properties, Synthesis, Characterization, and Applications*, IntechOpen, 2021.
7 C. Jiao, C. Dong, C. Xie, W. Luo, J. Zhang, S. Fan, Y. Liu, Y. Ma, X. He and Z. Zhang, Dissolution and retention process of CeO_2 nanoparticles in soil with dynamic redox conditions, *Environ. Sci. Technol.*, 2021, **55**, 14649–14657.
8 C. Jiao, C. Dong, W. Dai, W. Luo, S. Fan, L. Zhou, Y. Ma, X. He and Z. Zhang, Geochemical cycle of exogenetic CeO_2 nanoparticles in agricultural soil: Chemical transformation and re-distribution, *Nano Today*, 2022, **46**, 101563.
9 L. Xu, M. Xu, R. Wang, Y. Yin, I. Lynch and S. Liu, The crucial role of environmental coronas in determining the biological effects of engineered nanomaterials, *Small*, 2020, **16**, 2003691.
10 A. Gondikas, F. von der Kammer, R. Kaegi, O. Borovinskaya, E. Neubauer, J. Navratilova, A. Praetorius, G. Cornelis and T. Hofmann, Where is the nano? Analytical approaches for the detection and quantification of TiO_2 engineered nanoparticles in surface waters, *Environ. Sci.: Nano*, 2018, **5**, 313–326.
11 Z. Ban, P. Yuan, F. Yu, T. Peng, Q. Zhou and X. Hu, Machine learning predicts the functional composition of the protein corona and the cellular recognition of nanoparticles, *Proc. Natl. Acad. Sci. U. S. A.*, 2020, **117**, 10492–10499.
12 M. Ikram, R. Raees, A. Haider, A. Ul-Hamid, J. Haider, I. Shahzadi, W. Nabgan, S. Goumri-Said, M. B. Kanoun and S. Ali, Enhanced photocatalytic and antibacterial activity of TiO2 quantum dots doped with cerium/chitosan for environmental remediation: experimental and theoretical approaches, *Mater. Chem. Phys.*, 2023, **297**, 127462.

13 P. Wu, R. Xie, K. Imlay and J. K. Shang, Visible-light-induced bactericidal activity of titanium dioxide codoped with nitrogen and silver, *Environ. Sci. Technol.*, 2010, **44**, 6992–6997.
14 T. An, H. Zhao and P. K. Wong, *Advances in photocatalytic disinfection*, Springer, 2017.
15 Z. Qi, G. Li, M. Wang, C. Chen, Z. Xu and T. An, Photoelectrocatalytic inactivation mechanism of *E. coli* DH5α (TET) and synergistic degradation of corresponding antibiotics in water, *Water Res.*, 2022, **215**, 118240.
16 B. Ahmed, F. Ameen, A. Rizvi, K. Ali, H. Sonbol, A. Zaidi, M. S. Khan and J. Musarrat, Destruction of cell topography, morphology, membrane, inhibition of respiration, biofilm formation, and bioactive molecule production by nanoparticles of Ag, ZnO, CuO, TiO_2, and Al_2O_3 toward beneficial soil bacteria, *ACS Omega*, 2020, **5**, 7861–7876.
17 H. Yin, G. Li, X. Chen, W. Wang, P. K. Wong, H. Zhao and T. An, Accelerated evolution of bacterial antibiotic resistance through early emerged stress responses driven by photocatalytic oxidation, *Appl. Catal., B*, 2020, **269**, 118829.
18 M. Junaid and J. Wang, Interaction of nanoplastics with extracellular polymeric substances (EPS) in the aquatic environment: A special reference to eco-corona formation and associated impacts, *Water Res.*, 2021, **201**, 117319.
19 H. Yin, Y. Cai, G. Li, W. Wang, P. K. Wong and T. An, Persistence and environmental geochemistry transformation of antibiotic-resistance bacteria/genes in water at the interface of natural minerals with light irradiation, *Crit. Rev. Environ. Sci. Technol.*, 2022, **52**, 2270–2301.
20 L. Degenkolb, M. Kaupenjohann and S. Klitzke, The variable fate of Ag and TiO_2 nanoparticles in natural soil solutions—sorption of organic matter and nanoparticle stability, *Water, Air, Soil Pollut.*, 2019, **230**, 62.
21 X. Wang, T. Sun, H. Zhu, T. Han, J. Wang and H. Dai, Roles of pH, cation valence, and ionic strength in the stability and aggregation behavior of zinc oxide nanoparticles, *J. Environ. Manage.*, 2020, **267**, 110656.
22 L. Treuel, K. A. Eslahian, D. Docter, T. Lang, R. Zellner, K. Nienhaus, G. U. Nienhaus, R. H. Stauber and M. Maskos, Physicochemical characterization of nanoparticles and their behavior in the biological environment, *Phys. Chem. Chem. Phys.*, 2014, **16**, 15053–15067.
23 A. Kahru and H.-C. Dubourguier, From ecotoxicology to nanoecotoxicology, *Toxicology*, 2010, **269**, 105–119.
24 X. Yang, E. Chung, I. Johnston, G. Ren and Y.-K. Cheong, Exploitation of antimicrobial nanoparticles and their applications in biomedical engineering, *Appl. Sci.*, 2021, **11**, 4520.
25 H. Li, Y. Wang, Q. Tang, D. Yin, C. Tang, E. He, L. Zou and Q. Peng, The protein corona and its effects on nanoparticle-based drug delivery systems, *Acta Biomater.*, 2021, **129**, 57–72.
26 O. Metryka, D. Wasilkowski and A. Mrozik, Insight into the antibacterial activity of selected metal nanoparticles and alterations within the antioxidant defence system in *Escherichia coli*, *Bacillus cereus* and *Staphylococcus epidermidis*, *Int. J. Mol. Sci.*, 2021, **22**, 11811.
27 N. Behera, M. Arakha, M. Priyadarshinee, B. S. Pattanayak, S. Soren, S. Jha and B. C. Mallick, Oxidative stress generated at nickel oxide nanoparticle interface results in bacterial membrane damage leading to cell death, *RSC Adv.*, 2019, **9**, 24888–24894.
28 A. Ray Chowdhuri, S. Tripathy, S. Chandra, S. Roy and S. K. Sahu, A ZnO decorated chitosan–graphene oxide nanocomposite shows significantly enhanced antimicrobial activity with ROS generation, *RSC Adv.*, 2015, **5**, 49420–49428.
29 O. Metryka, D. Wasilkowski, M. Adamczyk-Habrajska and A. Mrozik, Undesirable consequences of the metallic nanoparticles action on the properties and functioning of *Escherichia coli*, *Bacillus cereus* and *Staphylococcus epidermidis* membranes, *J. Hazard. Mater.*, 2023, **446**, 130728.
30 M. Planchon, T. Léger, O. Spalla, G. Huber and R. Ferrari, Metabolomic and proteomic investigations of impacts of titanium dioxide nanoparticles on *Escherichia coli*, *PLoS One*, 2017, **12**, e0178437.
31 L. Gabrielyan, H. Badalyan, V. Gevorgyan and A. Trchounian, Comparable antibacterial effects and action mechanisms of silver and iron oxide nanoparticles on *Escherichia coli* and *Salmonella typhimurium*, *Sci. Rep.*, 2020, **10**, 13145.
32 O. Metryka, D. Wasilkowski and A. Mrozik, Evaluation of the effects of Ag, Cu, ZnO and TiO_2 nanoparticles on the expression level of oxidative stress-related genes and the activity of antioxidant enzymes in *Escherichia coli, Bacillus cereus* and *Staphylococcus epidermidis*, *Int. J. Mol. Sci.*, 2022, **23**, 4966.
33 J. Zhang, P. Su, H. Chen, M. Qiao, B. Yang and X. Zhao, Impact of reactive oxygen species on cell activity and structural integrity of Gram-positive and Gram-negative bacteria in electrochemical disinfection system, *Chem. Eng. J.*, 2023, **451**, 138879.
34 P. Bhattacharya, A. Dey and S. Neogi, An insight into the mechanism of antibacterial activity by magnesium oxide nanoparticles, *J. Mater. Chem. B*, 2021, **9**, 5329–5339.
35 P. P. Mahamuni-Badiger, P. M. Patil, M. V. Badiger, P. R. Patel, B. S. Thorat-Gadgil, A. Pandit and R. A. Bohara, Biofilm formation to inhibition: Role of zinc oxide-based nanoparticles, *Mater. Sci. Eng., C*, 2020, **108**, 110319.
36 M. G. Cusimano, F. Ardizzone, G. Nasillo, M. Gallo, A. Sfriso, D. Martino-Chillura, D. Schillaci, F. Baldi and G. Gallo, Biogenic iron-silver nanoparticles inhibit bacterial biofilm formation due to Ag+ release as determined by a novel phycoerythrin-based assay, *Appl. Microbiol. Biotechnol.*, 2020, **104**, 6325–6336.
37 J. Iqbal, A. Andleeb, H. Ashraf, B. Meer, A. Mehmood, H. Jan, G. Zaman, M. Nadeem, S. Drouet and H. Fazal, Potential antimicrobial, antidiabetic, catalytic, antioxidant and ROS/RNS inhibitory activities of Silybum marianum mediated biosynthesized copper oxide nanoparticles, *RSC Adv.*, 2022, **12**, 14069–14083.

38 A. G. Kicheeva, E. S. Sushko, L. S. Bondarenko, K. A. Kydralieva, D. A. Pankratov, N. S. Tropskaya, A. A. Dzeranov, G. I. Dzhardimalieva, M. Zarrelli and N. S. Kudryasheva, Functionalized magnetite nanoparticles: characterization, bioeffects, and role of reactive oxygen species in unicellular and enzymatic systems, *Int. J. Mol. Sci.*, 2023, **24**, 1133.

39 H. Y. Kwon, S. Y. Choi, M. H. Won, T.-C. Kang and J. H. Kang, Oxidative modification and inactivation of Cu,Zn-superoxide dismutase by 2,2′-azobis(2-amidinopropane) dihydrochloride, *Biochim. Biophys. Acta*, 2000, **1543**, 69–76.

40 Q. Liu, Y. Sun, M. Zhang and J. Hou, Comparison of *Escherichia coli* responses to different silver nanoparticles with different particle sizes and surface coatings, *Part. Part. Syst. Charact.*, 2024, **42**, 2400105.

41 E. Cabiscol, J. Tamarit and J. Ros, Oxidative stress in bacteria and protein damage by reactive oxygen species, *Int. Microbiol.*, 2000, **3**, 3–8.

42 C. Capasso and C. T. Supuran, Sulfa and trimethoprim-like drugs – antimetabolites acting as carbonic anhydrase, dihydropteroate synthase and dihydrofolate reductase inhibitors, *J. Enzyme Inhib. Med. Chem.*, 2014, **29**, 379–387.

43 A. Kamat and A. Badrinarayanan, SOS-independent bacterial DNA damage responses: diverse mechanisms, unifying function, *Curr. Opin. Microbiol.*, 2023, **73**, 102323.

44 Z. Baharoglu and D. Mazel, SOS, the formidable strategy of bacteria against aggressions, *FEMS Microbiol. Rev.*, 2014, **38**, 1126–1145.

45 A. Roy Chowdhury, S. Sah, U. Varshney and D. Chakravortty, Salmonella Typhimurium outer membrane protein A (OmpA) renders protection from nitrosative stress of macrophages by maintaining the stability of bacterial outer membrane, *PLoS Pathog.*, 2022, **18**, e1010708.

46 Y. Wang, Z. Bian and Y. Wang, Biofilm formation and inhibition mediated by bacterial quorum sensing, *Appl. Microbiol. Biotechnol.*, 2022, **106**, 6365–6381.

47 J. Wang, G. Li, H. Yin and T. An, Bacterial response mechanism during biofilm growth on different metal material substrates: EPS characteristics, oxidative stress and molecular regulatory network analysis, *Environ. Res.*, 2020, **185**, 109451.

48 P. Jawaid, M. U. Rehman, Q.-L. Zhao, M. Misawa, K. Ishikawa, M. Hori, T. Shimizu, J.-i. Saitoh, K. Noguchi and T. Kondo, Small size gold nanoparticles enhance apoptosis-induced by cold atmospheric plasma via depletion of intracellular GSH and modification of oxidative stress, *Cell Death Discovery*, 2020, **6**, 83.

49 W. Jiang, H. Mashayekhi and B. S. Xing, Bacterial toxicity comparison between nano- and micro-scaled oxide particles, *Environ. Pollut.*, 2009, **157**, 1619–1625.

50 A. Simon-Deckers, S. Loo, M. Mayne-L'hermite, N. Herlin-Boime, N. Menguy, C. Reynaud, B. Gouget and M. Carrière, Size-, Composition- and shape-dependent toxicological impact of metal oxide nanoparticles and carbon nanotubes toward bacteria, *Environ. Sci. Technol.*, 2009, **43**, 8423–8429.

51 S. V. Gudkov, D. E. Burmistrov, V. V. Smirnova, A. A. Semenova and A. B. Lisitsyn, A Mini Review of Antibacterial Properties of Al_2O_3 Nanoparticles, *Nanomaterials*, 2022, **12**, 2635.

52 O. Serdar, A. N. Aydin and I. C. Ç. Çimen, Determination of oxidative stress responses caused by aluminum oxide (γ-Al_2O_3 and α-Al_2O_3) nanoparticles in Gammarus pulex, *Chemosphere*, 2024, **352**, 141193.

53 S. Pakrashi, D. Kumar, V. Iswarya, M. Bhuvaneshwari, N. Chandrasekaran and A. Mukherjee, A comparative ecotoxicity analysis of α- and γ-phase aluminium oxide nanoparticles towards a freshwater bacterial isolate *Bacillus licheniformis*, *Bioprocess Biosyst. Eng.*, 2014, **37**, 2415–2423.

54 A. Boumaza, L. Favaro, J. Lédion, G. Sattonnay, J. B. Brubach, P. Berthet, A. M. Huntz, P. Roy and R. Tétot, Transition alumina phases induced by heat treatment of boehmite: An X-ray diffraction and infrared spectroscopy study, *J. Solid State Chem.*, 2009, **182**, 1171–1176.

55 V. Manikandan, P. Jayanthi, A. Priyadharsan, E. Vijayaprathap, P. M. Anbarasan and P. Velmurugan, Green synthesis of pH-responsive Al_2O_3 nanoparticles: Application to rapid removal of nitrate ions with enhanced antibacterial activity, *J. Photochem. Photobiol., A*, 2019, **371**, 205–215.

56 K. H. Jwad, T. H. Saleh and B. Abd-Alhamza, Preparation of aluminum oxide nanoparticles by laser ablation and a study of their applications as antibacterial and wounds healing agent, *Nano Biomed. Eng.*, 2019, **11**, 313–319.

57 Y. Liu, Z. Xu, M. Yin, H. Fan, W. Cheng, L. Lu, Y. Song, J. Ma and X. Zhu, Enhanced photoelectrocatalytic performance of α-Fe_2O_3 thin films by surface plasmon resonance of Au nanoparticles coupled with surface passivation by atom layer deposition of Al_2O_3, *Nanoscale Res. Lett.*, 2015, **10**, 374.

58 A. Zhu, S. Ali, Z. Wang, Y. Xu, R. Lin, T. Jiao, Q. Ouyang and Q. Chen, ZnO@Ag-functionalized paper-based microarray chip for SERS detection of bacteria and antibacterial and photocatalytic inactivation, *Anal. Chem.*, 2023, **95**, 18415–18425.

59 M. Baláž, L. Tkáčiková, M. Stahorský, M. Casas-Luna, E. Dutková, L. Čelko, M. Kováčová, M. Achimovičová and P. Baláž, Ternary and quaternary nanocrystalline cu-based sulfides as perspective antibacterial materials mechanochemically synthesized in a scalable fashion, *ACS Omega*, 2022, **7**, 27164–27171.